European Review for Medical and Pharmacological Sciences 2020; 24: 1956-1969

LncRNA ANRIL regulates cell proliferation and migration *via* sponging miR-339-5p and regulating FRS2 expression in atherosclerosis

T. HUANG[1], H.-Y. ZHAO[1], X.-B. ZHANG[2], X.-L. GAO[2], W.-P. PENG[2], Y. ZHOU[1], W.-H. ZHAO[1], H.-F. YANG[1]

[1]Department of Neurosurgery, Union Hospital, Tongji Medical College, Huazhong University of Science and Technology, Wuhan, China
[2]Department of Cardiology, Union Hospital, Tongji Medical College, Huazhong University of Science and Technology, Wuhan, China

Tao Huang and *Hongyang Zhao* are co-first authors

Abstract. – OBJECTIVE: Atherosclerosis (AS), with high risk of stroke or cerebrovascular disease, is one of the most common causes of death worldwide. Increasing evidence shows that long non-coding RNA (lncRNA) antisense non-coding RNA in the INK4 locus (ANRIL) is related to atherothrombotic stroke susceptibility and contributes to AS progression. However, the underlying mechanism was not explained yet.

PATIENTS AND METHODS: Human aorta vascular smooth muscle cells (HA-VSMCs) and human umbilical vein endothelial cells (HUVECs) were treated with oxidized Low Density Lipoprotein (ox-LDL) and considered as AS cell models. Quantitative reverse transcriptase PCR (qRT-PCR) and Western blotting were employed to investigate the mRNA and protein expression level, respectively. Microscopic examination through fluorescent in situ hybridization (FISH) was used to determine the location of ANRIL. Cell proliferation and migration assays were demonstrated to evaluate the functional role of ANRIL in AS. Potential target of ANRIL was determined using Luciferase reporter assay and RNA immunoprecipitation (RIP).

RESULTS: ANRIL was upregulated and miR-399-5p was down-regulated in both human atherosclerotic plaques and ox-LDL-induced cells. ANRIL was located in cytoplasm and promoted cell proliferation and migration by sponging miR-399-5p. Further analysis identified fibroblast growth factor receptor substrate 2 (FRS2) as a direct target of miR-399-5p. Finally, RAS/RAF/ERK signal pathway was proved to be involved in the regulation of ANRIL on the progression of AS.

CONCLUSIONS: These results revealed the underlying mechanism that ANRIL promoted AS progression by sponging miR-399-5p and regulating RAS/RAF/ERK signal pathway, suggesting that ANRIL might be a potential target for the therapeutic strategy of AS.

Key Words:
ANRIL, MiR-399-5p, FRS2, Atherosclerosis, Progression.

Introduction

Atherosclerosis (AS), a chronic inflammatory disease, is characterized by formation of atherosclerotic plaques in the aorta wall[1]. As the most common vasculopathy, AS could result in various diseases such as coronary artery disease, stroke or cerebrovascular disease[2,3], and is regarded as the leading cause of disability and death in the developed world[4]. Therefore, it is urgent to study the molecular pathogenesis of AS and explore effective therapeutic targets for AS treatment. Among different pathological events for AS, the migration and proliferation of endothelial cells (ECs) and vascular smooth muscle cells (VSMCs) are most commonly involved in the progression of AS[5,6]. In addition, an increase of low density lipoprotein (LDL), particularly oxidized LDL (ox-LDL), is considered as a significant and severe pathogenic factor for the development of AS[7,8].

Antisense non-coding RNA in the INK4 locus (ANRIL) is a long non-coding RNA that is located at chromosome 9p21.3[9]. It has been well investigated that ANRIL demonstrates an oncogenic role in the progression of non-small-cell lung cancer[10],

Corresponding Author: Haifeng Yang, MD; e-mail: HaifengYang139@163.com

esophageal squamous cell cancer[11], nasopharyngeal cancer[12], cervical cancer[13], and nasopharyngeal cancer[14]. Recently, strong relationships between chromosome 9p21.3 and cardiovascular disease have been reported[15-17], and the role of ANRIL in cardiovascular disease has been noted. Indeed, ANRIL was proved to be correlated with coronary heart disease[18,19]. Moreover, ANRIL was related to atherothrombotic stroke susceptibility in the Chinese population[20], and showed to be expressed in atheromatous vessels and vascular ECs[21]. Although ANRIL was found to be up-regulated in AS samples[22], the underlying mechanism of ANRIL in the regulation of AS is still unclear.

Generally, lncRNAs function in an intricate way[23,24], as a competing endogenous RNAs (ceRNAs) to sponging miRNAs, and thus affect the expression of target mRNA[25,26]. Here, our preliminary result indicated that ANRIL could bind to miR-339-5p. MiR-339-5p functions as a tumor suppressor gene in a variety of cancers, including breast cancer[27], colorectal cancer[28], non-small cell lung cancer[29], hepatocellular carcinoma[30], and ovarian cancer[31]. Moreover, miR-339 could inhibit the proliferation of pulmonary artery smooth muscle cells by targeting FGF signal pathway[32]. However, the functional role of miR-339-5p in the progression of AS is still unclear.

The aim of this study was to determine the role of ANRIL in AS and explore the underlying mechanism. HA-VSMCs and human umbilical vein endothelial cells (HUVECs) were treated with oxidized Low Density Lipoprotein (ox-LDL) and considered as AS cell models. Our results suggested that lncRNA ANRIL regulates cell proliferation and migration via sponging miR-339-5p and regulating FRS2 expression in atherosclerosis.

Patients and Methods

Total of 20 patients diagnosed pathologically and clinically with AS were recruited from the (cardiology) Department of Tongji Medical College. This research was approved by the Ethics Committee of Tongji Medical College. Atherosclerotic coronary tissues were collected from patients subjected to coronary endarterectomy and bypass grafting due to occlusive AS. For the same patients, internal mammary artery samples were collected during bypass surgery and used as controls. The demographic and clinical parameters of patients were summarized in Table I.

Cell Culture

Human embryonic kidney 293T (HEK-293T) cells, human aorta vascular smooth muscle cells (HA-VSMCs), and human umbilical vein endothelial cells (HUVECs) were purchased from

Table I. Demographic and clinical parameters of patients.

Patients, n.	20
Age, median (range)	59 (44-76)
Sex, male, n. (%)	15 (75%)
Smoking status	
Yes, n (%)	14 (70%)
No, n (%)	6 (30%)
Medical history	
Hyperlipidemia, n (%)	19 (95%)
Myocardial infarction, n (%)	10 (50%)
Diabetes mellitus, n (%)	9 (45%)
Hypertension, n (%)	17 (85%)
New York Heart Association (NYHA) Classification	
Class 2, n (%)	10 (50%)
Class 3, n (%)	8 (40%)
Class 4, n (%)	2 (10%)
Coronary arteries stenosis	
Right coronary artery, median (range)	75% (50-100)
Left anterior descending artery, median (range)	60% (40-80)
Circumflex artery, median (range)	65% (0-100)
Bypass (at least 1), n (%)	20 (100%)
Left ventricular ejection fraction, median (range)	40% (25-58)

American Type Culture Collection (ATCC; Manassas, VA, USA). The cells were cultured in Dulbecco's Modified Eagle's Medium (DMEM) containing 10% fetal bovine serum (FBS; Gibco, Life Technologies, Carlsbad, CA, USA) at an incubator with 37°C and 5% CO_2. HA-VSMCs and HUVECs cells with confluence of 80% were treated with different concentration of ox-LDL (0, 10, 25, 50 mg/L, Sigma-Aldrich, Saint Louis, MO, USA) for 48 h.

RNA-Fluorescence In Situ Hybridization (RNA-FISH)

To detect the intracellular location of ANRIL in ox-LDL-induced HA-VSMCs and HUVECs, the RNA-FISH procedure was performed as described in Biosearch Technologies (https://www.biosearchtech.com; Petaluma, CA, USA). Cells were firstly rinsed in PBS and fixed in 4% formaldehyde for 15 min at room temperature. Then, the cells were incubated with 0.1% Triton X-100 on ice for 10 min. Fluorescence-conjugated ANRIL probes were hybridized with the samples for 5 h in the dark at 37°C. DAPI was used to stain the nucleus. Laser scanning confocal microscopy (Carl Zeiss, Jena, Germany) was utilized to visualize the samples.

QRT-PCR

Sample RNAs were extracted from AS/healthy samples or ox-LDL-induced VSMCs and HUVECs via TRIzol reagent (Invitrogen, Carlsbad, CA, USA). MiRNAs were extracted using miRcute miRNA isolation kit (Tiangen, Beijing, China). The RNAs were then reverse transcribed into cDNAs using miScript Reverse Transcription kit (Qiagen, Hilden, Germany). cDNAs were amplified by using SYBR1 Premix Ex Taq™ II (TaKaRa, Otsu, Shiga, Japan). U6 was used as an internal reference and GAPDH as the endogenous controls. Three technological replicates were used to ensure the reliability. The primer sequences were showed: ANRIL, 5'-TTATGCTTTGCAGCACACTGG-3' (forward) and 5'-GTTCTGCCACAGCTTTGATCT-3' (reverse); miR-339-5p, 5'-GGGTCCCTGTCCTCCA-3' (forward) and 5'-TGCGTGTCGTGGAGTC-3' (reverse); FRS2, 5'-GGCTGAGACTCGATCTGCTCCAA-3' (forward) and 5'-GGCGCGAACCCCCAGACT-3' (reverse); U6, 5'-CTCGCTTCGGCAGCACA-3' (forward) and 5'-AACGCTTCACGAATTTGCGT-3' (reverse); GAPDH, 5'-TGTTCGTCATGGGTGTGAAC-3' (forward) and 5'-ATGGCATGGACTGTGGTCAT-3' (reverse).

Cell Viability Assay

100 µL 5 × 10^3 ox-LDL-induced VSMCs and HUVECs in each group per well were cultured in 96-well plates for 24 h and then were treated with Anlotinib for another 24 h. CCK-8 assay (Solarbio, Beijing, China) was utilized to estimate cell viability, and calculated by means of spectrophotometric plate reader (BioTek, Winooski, VT, USA) at 450 nm. All the results were tested at least three independent experiments.

Flow Cytometry

1×10^4 cells/well ox-LDL-induced VSMCs and HUVECs were harvested and washed with PBS. The cells were then fixed with 70% ethanol at 4°C for at least 30 min. After washing with PBS, ribonuclease (Abcam, Cambridge, MA, USA) was added to the cells, and the propidium iodide (PI, 200 µL, Abcam, Cambridge, MA, USA) was used to stain the cells. FACS flow cytometer (Attune, Life Technologies, Darmstadt, Germany) was used to analyze cell cycle.

Cell Migration Assay

In vitro wound healing assay was utilized to assess the migration of ox-LDL-induced VSMCs and HUVECs. 1×10^6 cells per well were seeded into 6-well plates for 24 h. The wound gaps were formed by gently scratching with a pipette. The cells were then cultured in DMEM for another 24 h before calculating the wound width under an inverted microscope.

Luciferase Reporter Assay

The fragments of 3'UTR of ANRIL and FRS2 containing the binding site were amplified by PCR and cloned into psi-CHECK™-2 vector (Promega, Madison, WI, USA), respectively. 2×10^3 HEK-293T cells per well were seeded in 48-well plates for 24 h. Cells were then transfected with psiCHECK-™-2-ANRIL or FRS2 3'UTR and psiCHECK-™-2-mut-ANRIL or FRS2 3'UTR in combination with miR-339-5p mimics, inhibitor or the negative control (80 nM; GenePharma, Shanghai, China) by Lipofectamine 2000 (Invitrogen, Carlsbad, CA, USA). 48 h later, Luciferase activities were measured using the Dual-Luciferase Reporter Assay System (Promega, Madison, WI, USA). Firefly Luciferase activity was normalized to *Renilla* Luciferase activity for each group.

Plasmid Construction and Transfection

For ANRIL overexpression, the plasmid pcDNA™3.1 (Invitrogen, Carlsbad, CA, USA) was

designed to construct pcDNA3.1-ANRIL. For ANRIL knockdown, two small interfering RNAs for ANRIL (si-ANRIL#1, si-ANRIL#2) and the negative control (si-NC) were synthesized from GenePharma. For transient pcDNA3.1-ANRIL, siRNAs or miRNAs transfection, 3×10^4 ox-LDL-induced VSMCs and HUVECs cells per well were seeded in 12-well plates for 24 h in culture medium. The cells were then transfected with 200 nM pcDNA3.1-ANRIL, siRNAs or miRNAs by Lipofectamine 2000.

RNA Immunoprecipitation (RIP)

Ox-LDL-induced VSMCs and HUVECs cells transfected with pcDNA3.1-ANRIL were collected and lysed, and then incubated with protein G Sepharose beads (GE Healthcare, Eindhoven, The Netherlands) coated with anti-AGO2 antibody (Abcam, Cambridge, MA, USA) at 4°C overnight, and anti-IgG antibody was used as the negative control. RNA was then isolated for qRT-PCR as mentioned before.

Western Blot

Cultured or transfected ox-LDL-induced VSMCs and HUVECs were harvested and lysed in RIPA buffer (KeyGen, Nanjing, China). Protein lysates were loaded onto 10% sulphate-polyacrylamide gel electrophoresis (SDS-PAGE), and then transferred to polyvinylidene difluoride (PVDF) membrane. The membrane was blocked in PBS-T with 5% bovine serum albumin (BSA) for 2 h. PVDF membranes were then probed with rabbit anti-FRS2 monoclonal antibody (1:800, Abcam, Cambridge, MA, USA), Ras, Raf, p-Raf, ERK1/2, p-ERK1/2 monoclonal antibody (1:1000, Abcam, Cambridge, MA, USA), β-actin (1:2000, Abcam, Cambridge, MA, USA) overnight at 4°C. The PVDF membrane was washed with TBST (10 min × 3 times) and labeled with horseradish peroxidase (HRP)-conjugated secondary antibodies (1:5000; Abcam, Cambridge, MA, USA) for 1 h. Immunoreactivities were detected by enhanced chemiluminescence (ECL; KeyGen, Nanjing, China). β-actin was used as a control.

Statistical Analysis

All results were expressed as mean ± SEM of at least 3 independent experiments. GraphPad Prism software (GraphPad Prism Software Inc., San Diego, CA, USA) and one-way analysis of variance (ANOVA) were used for statistical analyses. $p < 0.05$, $p < 0.01$ or $p < 0.001$ were considered as statistically significant.

Results

Negative Relationship Between ANRIL Expression and MiR-339-5p Level in AS Patients and ox-LDL- Induced VSMCs and HUVECs

To identify the functional role of ANRIL and miR-339-5p in the progression of AS, qRT-PCR analysis was performed in human atherosclerotic plaques and ox-LDL-induced HA-VSMCs and HUVECs. As showed in Figure 1A, ANRIL was significantly up-regulated in human atherosclerotic plaques (AS) compared to non-atherosclerotic arteries (Normal) (n=20, $p < 0.001$), while miR-339-5p was down-regulated in AS group (Figure 1B). The correlation analysis suggested a negative correlation between ANRIL expression and miR-339-5p level (Figure 1C). Moreover, in ox-LDL-induced VSMCs and HUVECs, the expression of ANRIL was markedly induced by ox-LDL treatment in a dose- and time-dependent manner (Figure 1D, E). On the contrary, the expression of miR-339-5p in HA-VSMCs and HUVECs was significantly inhibited by ox-LDL treatment in a dose- and time-dependent manner (Figure 1F-1G). These results indicated that ANRIL was up-regulated and miR-339-5p was down-regulated both in *in vivo* and *in vitro*.

According to RNA-fluorescence *in situ* hybridization (RNA-FISH) assay, we discovered that ANRIL was located in the cytoplasm of VSMCs and HUVECs (Figure 1H), and 50 μg/mL of ox-LDL treatment induced the expression of ANRIL (Figure 1H). Furthermore, CCK-8 assay showed that 50 μg/mL of ox-LDL treatment increased the viability of VSMCs and HUVECs (Figure 1I), and wound healing assay detected ox-LDL treatment promoted the migration of VSMCs and HUVECs (Figure 1J).

ANRIL Directly Bind to MiR-339-5p and Negatively Regulated its Expression

Emerging evidence has shown that lncRNA is a molecular sponge that modulates the expression and function of miRNAs. The StarBase (http://starbase.sysu.edu.cn/) analysis predicted ANRIL may harbor potential binding sites to miR-339-5p (Figure 2A). RIP analysis demonstrated a strong enrichment of miR-339-5p in both ox-LDL-induced VSMCs (Figure 2B) and HUVECs (Figure 2C) that transfected with ANRIL overexpression vector, pcDNA-ANRIL. Moreover, Luciferase reporter assay showed that miR-339-5p mimics dramatically decreased the Luciferase activity of reporter gene with wild-type ANRIL 3'UTR

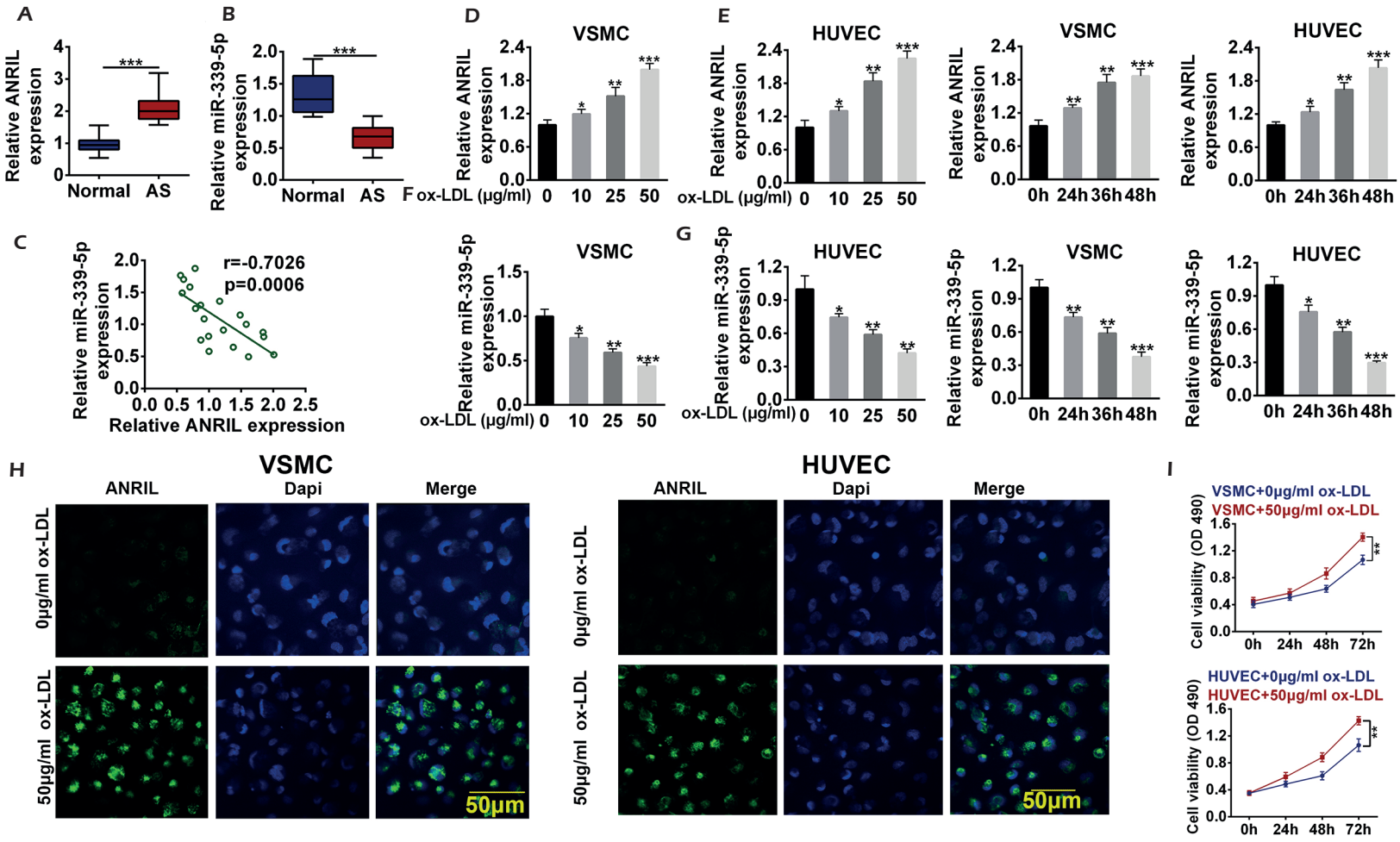

Figure 1. Negative relation between ANRIL and miR-339-5p in AS patients and ox-LDL-induced VSMCs and HUVECs. **A,** QRT-PCR analysis of ANRIL in human atherosclerotic plaques (AS) and normal healthy people (Normal). *** AS *vs.* Normal, $p < 0.001$. **B,** QRT-PCR analysis of miR-339-5p in human atherosclerotic plaques (AS) and normal healthy people (Normal). *** AS *vs.* Normal, $p < 0.001$. **C,** Negative correlation between ANRIL and miR-339-5p. **D,** QRT-PCR analysis of ANRIL in different concentration of ox-LDL-induced HA-VSMCs and HUVECs. *, **, *** 10, 20, 50 μg/mL *vs.* 0 μg/mL, $p < 0.05$, $p < 0.01$, $p < 0.001$. **E,** QRT-PCR analysis of ANRIL in different treatment time of 50 μg/Ml ox-LDL-induced HA-VSMCs and HUVECs. *, **, *** 48, 36, 24 h *vs.* 0 h, $p < 0.05$, $p < 0.01$, $p < 0.001$. **F,** QRT-PCR analysis of miR-339-5p in different concentration of ox-LDL-induced HA-VSMCs and HUVECs. *, **, *** 10, 20, 50 μg/mL *vs.* 0 μg/mL, $p < 0.05$, $p < 0.01$, $p < 0.001$. **G,** QRT-PCR analysis of miR-339-5p in different treatment time of 50 μg/mL ox-LDL-induced HA-VSMCs and HUVECs. *, **, *** 48, 36, 24 h vs. 0 h, $p < 0.05$, $p < 0.01$, $p < 0.001$. **H,** RNA-FISH detect the expression and location of ANRIL in VSMCs and HUVECs (magnification × 400). **I,** Ox-LDL treatment increased the cell viability of ox-LDL induced VSMCs and HUVECs. ** 50 μg/mL *vs.* 0 μg/mL, $p < 0.01$. **J,** Ox-LDL treatment promoted migration of ox-LDL induced VSMCs and HUVECs (Scan Bar 100 μm). **, *** 50 μg/mL *vs.* 0 μg/mL, $p < 0.01$, $p < 0.001$.

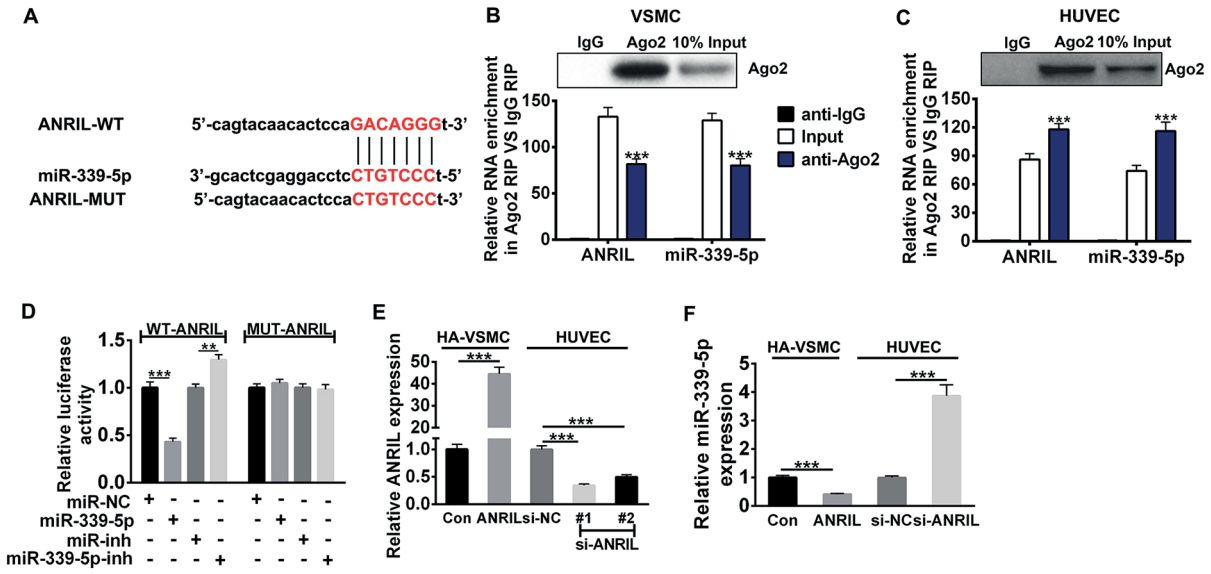

Figure 2. ANRIL directly bind with and negatively regulated expression of miR-339-5p. **A,** Potential binding site for miR-339-5p in ANRIL. **B,** RIP assay demonstrated a strong enrichment of miR-339-5p by ANRIL over-expression in ox-LDL-induced VSMCs. **C,** RIP assay demonstrated a strong enrichment of miR-339-5p by ANRIL over-expression in ox-LDL-induced HUVECs. *** Ago2 *vs.* IgG, $p < 0.001$. **D,** Luciferase reporter assay of miR-339-5p mimics (miR-339-5p), miR-339-5p inhibitor (miR-339-5p-inh) and their negative control with wild-type or mutant ANRIL. ***miR-339-5p vs. miR-NC, $p < 0.001$. ** miR-339-5p-inh vs. miR-inh, $p < 0.01$. **E,** Transfection efficiency of pcDNA-ANRIL (ANRIL) or si-ANRIL #1/#2 were detected via qRT-PCR in ox-LDL induced VSMCs and HUVECs. *** ANRIL *vs.* Con or siANRIL *vs.* si-NC, $p < 0.001$. **F,** Effect of pcDNA-ANRIL (ANRIL) or si-ANRIL #1/#2 on the expression of miR-339-5p in ox-LDL induced VSMCs and HUVECs. *** ANRIL *vs.* Con or siANRIL *vs.* si-NC, $p < 0.001$.

compared with negative control ($p < 0.001$), while miR-339-5p inhibitor increased the Luciferase activity (Figure 2D). These investigations indicated ANRIL could directly bind to miR-339-5p.

Afterwards, pcDNA-ANRIL was transfected into VSMCs, and HUCECs were transfected with si-ANRIL #1/#2, and the transfection efficiency was confirmed by qRT-PCR (Figure 2E). Particularly, the expression of ANRIL was lower in HUCECs that transfected with si-ANRIL #1 as compared to that transfected with si-ANRIL #2 and was thus selected for the following experiments and named as si-ANRIL. Additionally, qRT-PCR analysis confirmed that ANRIL over-expression significantly down-regulated miR-339-5p expression (Figure 2F), and ANRIL knockdown markedly increased miR-339-5p expression (Figure 2F). These findings showed that ANRIL negatively regulated miR-339-5p expression.

ANRIL Promoted the Proliferation and Migration of ox-LDL-Induced VSMCs and HUVECs Through Targeting MiR-339-5p

To determine whether miR-339-5p was involved in the functional role of ANRIL in AS, miR-339-5p mimics or inhibitor was transfected into VSMCs and HUVECs, respectively (Figure 3A). Of note, miR-339-5p mimics significantly reversed the ANRIL over-expression induced enhancement in viability in ox-LDL-induced VSMCs (Figure 3B). Inversely, si-ANRIL increased the suppressed cell viability by miR-339-5p inhibitor in ox-LDL-induced HUVECs (Figure 3B). Flow cytometry demonstrated that ANRIL over-expression decreased the percentage of ox-LDL-induced VSMCs in G1 phrase and increased the percentage of ox-LDL-induced VSMCs in S phrase, but miR-339-5p mimics markedly reversed these results (Figure 3C). ANRIL knockdown suppressed the cell cycle at G1 phase and miR-339-5p inhibitor reversed its inhibitive effect on ox-LDL-induced HUVECs (Figure 3C). Furthermore, wound healing assay confirmed the simulative role of ANRIL in the migration of ox-LDL-induced VSMCs was significantly attenuated by miR-339-5p mimics (Figure 3D). Similarly, the inhibitive role of si-ANRIL in the migration of ox-LDL-induced HUVECs was also markedly attenuated by miR-339-5p inhibitor (Figure 3D).

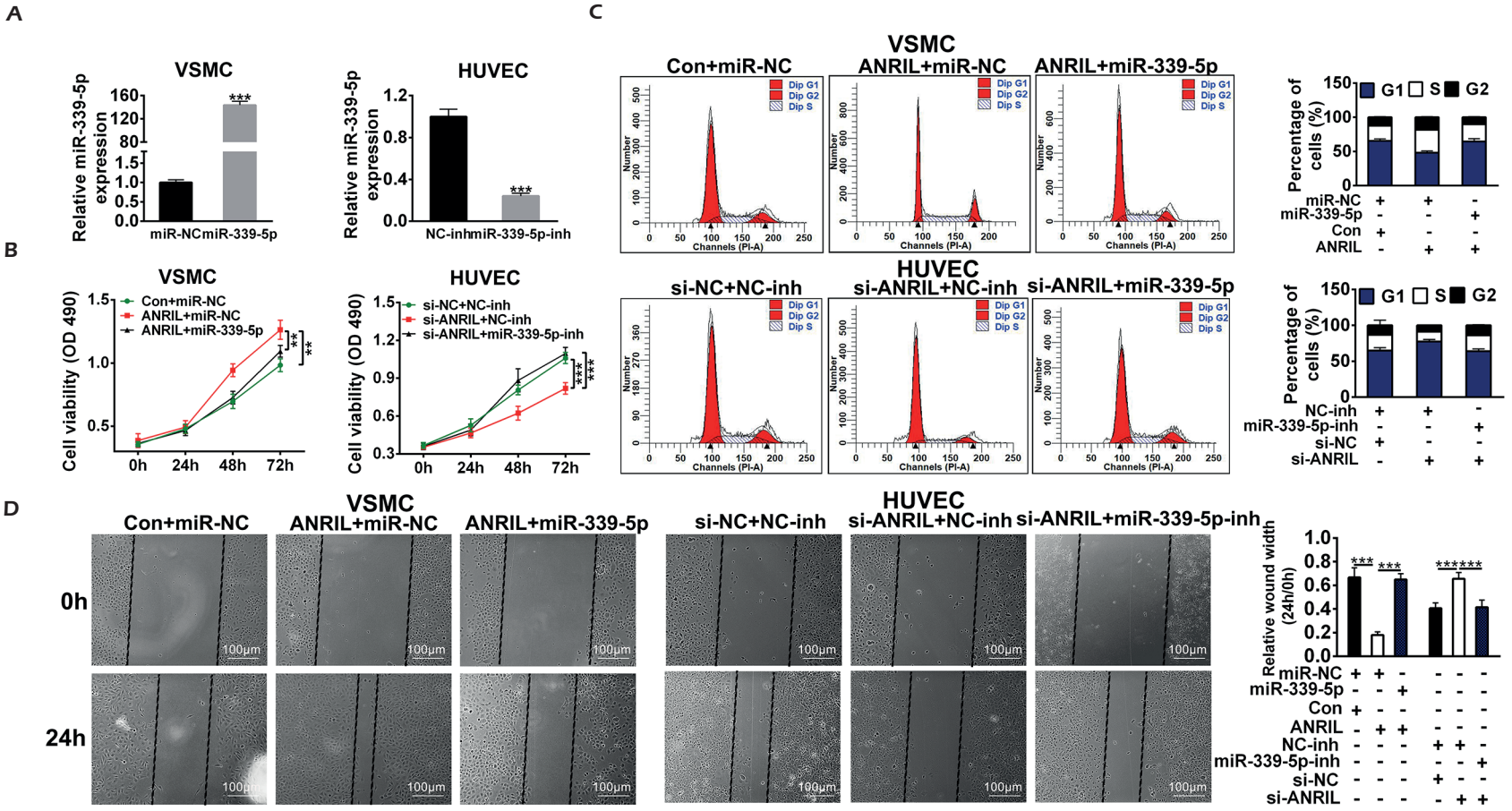

Figure 3. ANRIL promoted the proliferation and migration of ox-LDL-induced VSMCs and HUVECs through targeting miR-339-5p. **A,** Transfection efficiency of miR-339-5p mimics and inhibitor in ox-LDL induced VSMCs and HUVECs.***miR-339-5p *vs.* miR-NC or miR-339-5p-inh *vs.* miR-inh, $p < 0.001$. **B,** Effect of ANRIL and miR-339-5p on the cell viability of ox-LDL induced VSMCs and HUVECs. **ANRIL + miR-339-5p or Con + miR-NC *vs.* ANRIL + miR-NC, $p < 0.01$. *** siANRIL + miR-339-5p-inh or si-NC + NC-inh *vs.* si-ANRIL + NC-inh, $p < 0.001$. **C,** Effect of ANRIL and miR-339-5p on the cell cycle of ox-LDL induced VSMCs and HUVECs. **D,** Effect of ANRIL and miR-339-5p on the migration of ox-LDL induced VSMCs and HUVECs (Scan Bar 100 μm). *** ANRIL + miR-339-5p or Con + miR-NC *vs.* ANRIL + miR-NC, $p < 0.001$. *** siANRIL + miR-339-5p-inh or si-NC + NC-inh *vs.* si-ANRIL + NC-inh, $p < 0.001$.

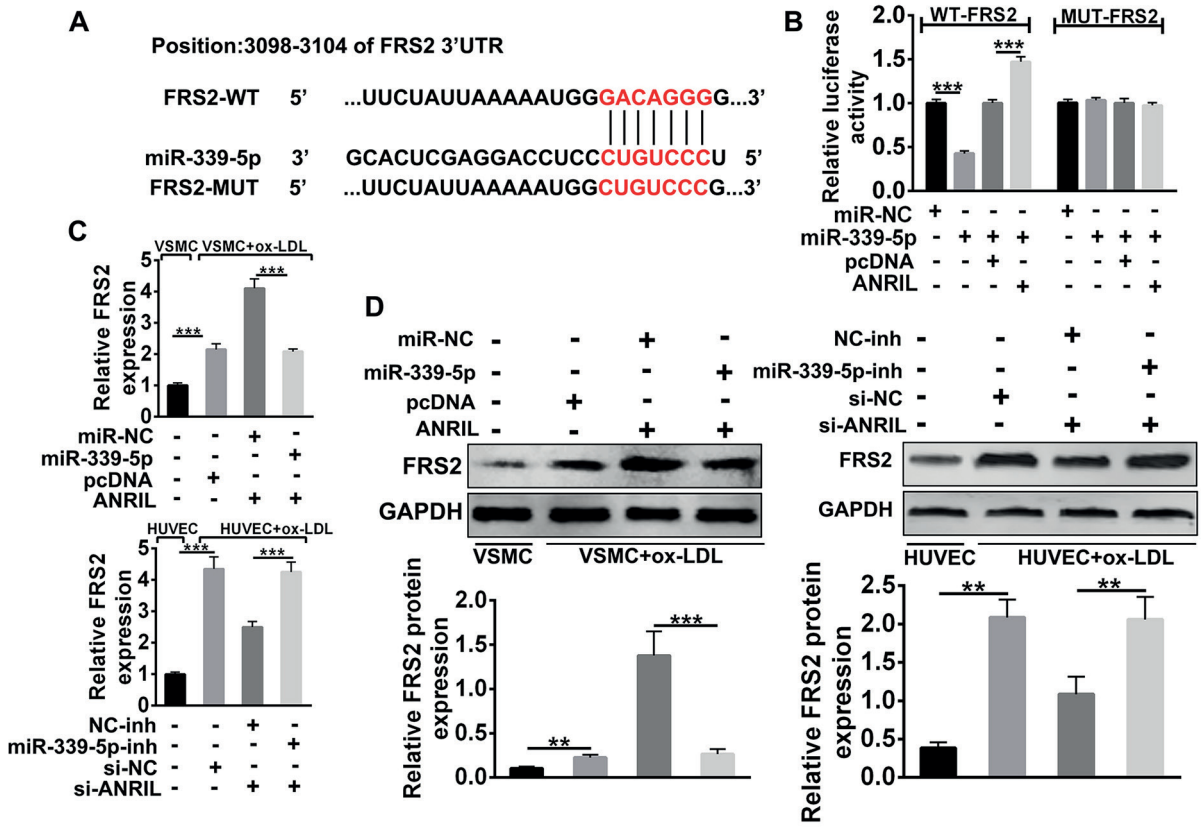

Figure 4. ANRIL regulated the expression of FRS2 via miR-339-5p. **A,** Potential binding site for miR-339-5p in 3'UTR of FRS2. **B,** Luciferase reporter assay of miR-339-5p mimics (miR-339-5p) and ANRIL over-expression (ANRIL) with wild-type or mutant FRS2. *** miR-339-5p *vs.* miR-NC, $p < 0.001$. ***ANRIL *vs.* Con, $p < 0.001$. **C,** Effect of mi-339-5p mimics or inhibitor, pcDNA-ANRIL (ANRIL) or si-ANRIL on the mRNA expression of FRS2 in VSMCs and HUVECs or ox-LDL induced VSMCs and HUVECs. *** ox-LDL induced VSMCs or HUVECs *vs.* VSMCs or HUVECs, $p < 0.001$.*** ANRIL + miR-339-5p *vs.* ANRIL + miR-NC, $p < 0.001$.*** si-ANRIL + miR-339-5p-inh vs. si-ANRIL + NC-inh, $p < 0.001$. **D,** Effect of mi-339-5p mimics or inhibitor, pcDNA-ANRIL (ANRIL) or si-ANRIL on the protein expression of FRS2 in VSMCs and HUVECs or ox-LDL induced VSMCs and HUVECs. ** ox-LDL induced VSMCs or HUVECs *vs.* VSMCs or HUVECs, $p < 0.01$. *** ANRIL + miR-339-5p v*s*. ANRIL + miR-NC, $p < 0.001$.** si-ANRIL + miR-339-5p-inh *vs*. si-ANRIL + NC-inh, $p < 0.01$.

ANRIL Regulated the Expression of FRS2 Via MiR-339-5p

During FGF signal transduction, fibroblast growth factor receptor substrate 2 (FRS2) is a key adaptive protein to regulate the growth, migration, and phenotypic plasticity of VSMCs[33]. Besides, FRS2 was predicted as a downstream mRNA for miR-339-5p via Targetscan (http://www.targetscan.org/mamm_31/) (Figure 4A). Luciferase reporter assay confirmed that miR-339-5p could bind to FRS2. Briefly, miR-339-5p mimics significantly decreased the Luciferase activity of reporter gene with wild-type FRS2 3'UTR compared to negative control, but the Luciferase activity was increased after pcDNA-ANRIL transfection (Figure 4B). Nevertheless, the regulatory effect of miR-455-3p mimics and pcDNA-ANRIL was inhibited when the predicted miR-339-5p-binding site in 3'UTR of FRS2 was mutated (Figure 4B). The results also showed that ox-LDL treatment significantly increased the mRNA and protein expression of FRS2 in VSMCs (Figure 4C, D). Besides, in ox-LDL-induced VSMCs, over-expression of ANRIL promoted the mRNA and protein expression level of FRS2, but miR-339-5p mimics decreased the mRNA and protein expression of FRS2 (Figure 4C, D). Similarly, ox-LDL treatment also increased the mRNA and protein expression of FRS2 in HUVECs (Figure 4C, D). In ox-LDL-induced HUVECs, ANRIL knockdown decreased the mRNA and protein expression of FRS2 and miR-339-5p inhibitor showed contrary results (Figure 4C, D). In general, these findings revealed that ANRIL act as a molecular sponge

1963

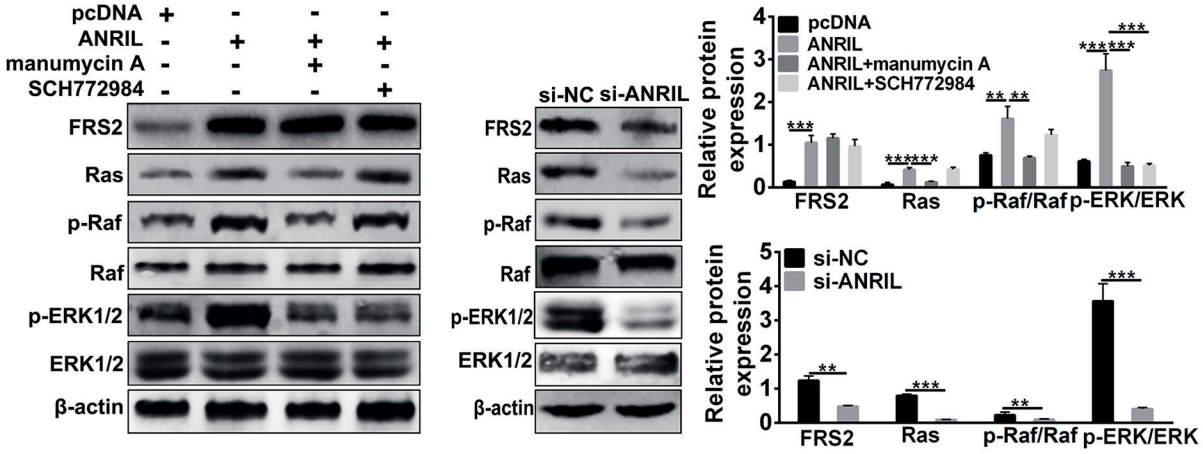

Figure 5. ANRIL promoted proliferation and migration of ox-LDL-induced VSMCs and HUVECs *via* RAS/RAF/ERK signaling pathway. Effect of ANRIL, si-ANRIL, manumycin A and SCH772984 on regulation of FRS2, Ras, Raf, p-Raf, ERK 1/2 and p-ERK 1/2 expression. **, *** ANRIL vs. Con, $p < 0.01$, $p < 0.001$. **, *** ANRIL *vs.* ANRIL + manumycin A or ANRIL + SCH772984, $p < 0.01$, $p < 0.001$. **, *** si-ANRIL vs. si-NC, $p < 0.01$, $p < 0.001$.

of miR-339-5p, and regulated FRS2 expression in ox-LDL-induced VSMCs and HUVECs.

ANRIL Promoted Proliferation and Migration of ox-LDL-Induced VSMCs and HUVECs Via RAS/RAF/ERK Signaling Pathway

It is well established that activation of RAS/RAF/ERK signaling pathway is involved in the proliferation and migration of VSMCs[34,35], thus we detected whether ANRIL could regulate RAS/RAF/ERK signaling pathway. Manumycin A and SCH772984 (an ERK inhibitor) were used to inhibit the downstream respective receptor of RAS/RAF/ERK signaling pathway. As shown in Figure 5, over-expression of ANRIL increased the expression of FRS2, Ras, Raf, p-Raf, ERK 1/2, p-ERK 1/2, as well as the ratio of p-Raf/Raf and p-ERK 1/2/ERK 1/2, suggesting the activation of RAS/RAF/ERK pathway. Manumycin A or SCH772984 treatment decreased the expression of Ras, the ratio of p-Raf/Raf and p-ERK 1/2/ERK 1/2, demonstrating an inhibitory effect on the signal pathway (Figure 5). Moreover, knockdown of ANRIL in ox-LDL-induced HUVECs not only decreased FRS2 expression, but also decreased the expression of Ras, Raf, p-Raf, ERK 1/2, p-ERK 1/2, as well as the ratio of p-Raf/Raf and p-ERK 1/2/ERK 1/2 (Figure 5). These results indicated that the effect of ANRIL on inducing RAS/RAF/ERK signaling pathway may be partially due to its inhibitive effects on the expression of FRS2, thus influenced the proliferation and migration of ox-LDL-induced VSMCs and HUVECs.

Discussion

It has been well-known that a large number of lncRNAs and miRNAs were highly expressed in cerebrovascular endothelium[36-38], serving as critical mediators to regulate cerebral vascular function and finally mediate cerebrovascular disease[39,40]. Zhang et al[41] have suggested that ANRIL was closely associated with AS and considered as a novel marker for atherothrombotic stroke. ANRIL transcripts were significantly up-regulated in human atherosclerotic plaque tissues[42]. Loss of function via siRNAs targeting ANRIL regulated the genes correlated with cell proliferation and extra-cellular matrix remodeling to finally affect atherogenic pathways[43]. Although ANRIL was shown to contribute to the risk of ischemic stroke[44], and bind with polycomb repression complex-1 (PRC-1) and PRC-2[45,46] to regulate cellular life span, the detailed functional role of ANRIL in the pathogenesis of AS remains under-investigated. We provide evidence that ANRIL acts as a miR-339-5p sponge and molecular regulator of FRS2 and RAS/RAF/ERK signaling pathway, which consequently participates in the progression of AS.

We firstly demonstrated up-regulation of ANRIL in AS patient, showing its potential role in

the progression of AS. Ox-LDL could induce AS by promoting ECs dysfunction and modulating VSMCs behavior[47,48]. VSMC is not only a major cell type in blood vessels, but also considered as an essential component of vascular system[49,50]. Therefore, ox-LDL-induced HA-VSMCs and HUVECs are widely used as *in vitro* cell models of AS. Here, ANRIL was also up-regulated in the *in vitro* cell models of AS.

Abnormal proliferation and migration of VSMCs could affect blood pressure, and play an important role in arterial wall remodelling to keep blood flow in AS-affected vessels[51-53]. Therefore, suppressing proliferation and migration of VSMC is recognized as a key therapeutic strategy for ameliorating AS. Knockdown of lncRNA homeoboxA11 antisense RNA (HOXA11-AS) could inhibit the proliferation and migration of VSMCs, which was beneficial for AS[54]. LncRNA TUG1 was closely related to the progression of AS via promoting proliferation of VSMCs, and knockdown of TUG1 inhibited proliferation of VSMCs[55]. In the present study, ox-LDL treatment induced cell viability and migration of HA-VSMCs and HUVECs. ANRIL over-expression promoted proliferation and migration of ox-LDL-induced HA-VSMCs and HUVECs, and knockdown of ANRIL lead to completely inverse results. Consistently, previous researches[56,57] found that ANRIL overexpression induced proliferation of VSMCs via NF-κB signaling pathways. ANRIL was shown to induce proliferation and inhibit apoptosis of human coronary endothelial cells (HCAECs) and HUVECs in a miR-181b-dependent manner in coronary artery disease[58]. The following Luciferase assay, RIP and qRT-PCR assays confirmed that ANRIL could negatively regulate miR-339-5p expression. Functional assays also showed that ANRIL knockdown-mediated anti-migration and anti-proliferation effects were suppressed via miR-339-5p inhibitor in ox-LDL induced HA-VSMCs and HUVECs.

FRS2 was characterized as a potential target of miR-339-5p, confirmed by the subsequent Luciferase assay. In pulmonary artery smooth muscle cell, FRS2 was determined as a target of miR-339, and miR-339 inhibited cell proliferation via FGF signaling pathway[32]. We revealed that ANRIL functioned as a molecular sponge of miR-339-5p to consequently increase FRS2 expression in ox-LDL induced HA-VSMCs and HUVECs. Through the N-terminal phosphotyrosine-binding domain, FRS2 binds to FGFR, and subsequently activate downstream RAS/RAF/ERK signaling pathway to regulate cell proliferation[59]. Moreover, RAS/RAF/ERK signaling has been shown as important regulating pathway in cardiovascular health and disease[60], and activation of RAS/RAF/ERK is involved in AS by inducing senescence of VSMCs and secretion of proinflammatory cytokines[61]. Some studies[62,35] also showed that disruption of RAS/RAF/ERK pathway resulted in the suppression of coronary artery endothelial tube formation and inhibition of VSMCs proliferation. Therefore, the effects of ANRIL/miR-339-5p on the expressions of RAS/RAF/ERK pathway-related genes (RAS, RAF, p-RAF, ERK1/2, p-ERK1/2) were measured in ox-LDL induced HA-VSMCs and HUVECs. Results showed that over-expression of ANRIL blocked miR-339-5p expression, and miR-339-5p down-regulation activated RAS/RAF/ERK signaling pathway. Besides, the induced role of anti-miR-339-5p on RAS/RAF/ERK signaling pathway was abolished by ANRIL knockdown, thus inhibiting proliferation and migration of ox-LDL-induced VSMCs and HUVECs.

In addition to the linear structure of ANRIL, circular non-coding RNA ANRIL (cANRIL) has also been confirmed to regulate AS via modulation of ribosomal RNA maturation[63] and inflammatory response of vascular ECs[9]. Notably, cANRIL showed a protective effect on AS[57], just the opposite to linear ANRIL. Moreover, macrophages that accumulate in atherosclerotic plaques appear to have a diminished capacity to migrate, which participate in the inflammatory process and play a key role in the pathogenesis of AS[64-66]. Otherwise, the effect of ANRIL on AS is not only involved in cell proliferation and migration, but also it may be related to the inflammatory process[57]. Therefore, due to different transcripts of ANRIL and complicated pathogenesis of AS, the effect of ANRIL on macrophages and inflammation, along with the detailed underlying molecular mechanisms, need to be further explored. Moreover, further analysis on the effects of ANRIL on regulating AS is still indispensable to be investigated in animal models.

Conclusions

The above data demonstrated that lncRNA ANRIL knockdown inhibited proliferation and migration of ox-LDL induced HA-VSMCs and HUVECs by sponging miR-339-5p and inactivating the RAS/RAF/ERK signaling pathway. These finding

illuminated the relation between ANRIL/miR-339-5p/FRS2 regulatory axis and ox-LDL-induced HA-VSMCs and HUVECs progression, suggesting potential application of ANRIL in AS treatment.

Conflict of Interests

The Authors declare that they have no conflict of interests.

Funding

This work was supported by National Natural Science Foundation of China (Grant No. 81701166) to Haifeng Yang.

References

1) Libby P. Inflammation in atherosclerosis. Nature 2002; 420: 868-874.
2) Choromanska B, Mysliwiec P, Choromanska K, Dadan J, Chabowski A. The role of CD36 receptor in the pathogenesis of atherosclerosis. Adv Clin Exp Med 2017; 26: 717-722.
3) Millen AE, Nie J, Sahli MW, Mares J A, Meyers KJ, Klein BEK, LaMonte MJ, Lutsey PL, Andrews CA, Klein R. Vitamin D status and prevalent early age-related macular degeneration in African Americans and Caucasians: the atherosclerosis risk in communities (ARIC) study. J Nutr Health Aging 2017; 21: 772-780.
4) Tofield A. ESC CardioMed: the new ESC Textbook of Cardiovascular Medicine, an innovative digital textbook database for today's cardiologists from the European Society of Cardiology will soon be available. Eur Heart J 2017; 38: 3252-3253.
5) Stocker R, Keaney J F, Jr. Role of oxidative modifications in atherosclerosis. Physiol Rev 2004; 84: 1381-1478.
6) Obikane H, Abiko Y, Ueno H, Kusumi Y, Esumi M, Mitsumata M. Effect of endothelial cell proliferation on atherogenesis: a role of p21(Sdi/Cip/Waf1) in monocyte adhesion to endothelial cells. Atherosclerosis 2010; 212: 116-122.
7) Bisgaard LS, Mogensen CK, Rosendahl A, Cucak H, Nielsen LB, Rasmussen SE, Pedersen TX. Bone marrow-derived and peritoneal macrophages have different inflammatory response to oxLDL and M1/M2 marker expression - implications for atherosclerosis research. Sci Rep 2016; 6: 35234.
8) Di Pietro N, Formoso G, Pandolfi A. Physiology and pathophysiology of oxLDL uptake by vascular wall cells in atherosclerosis. Vascul Pharmacol 2016; 84: 1-7.
9) Song CL, Wang JP, Xue X, Liu N, Zhang XH, Zhao Z, Liu JG, Zhang CP, Piao ZH, Liu Y, Yang YB. Effect of circular ANRIL on the inflammatory response of vascular endothelial cells in a rat model of coronary atherosclerosis. Cell Physiol Biochem 2017; 42: 1202-1212.
10) Nie FQ, Sun M, Yang JS, Xie M, Xu TP, Xia R, Liu YW, Liu XH, Zhang EB, Lu KH, Shu YQ. Long noncoding RNA ANRIL promotes non-small cell lung cancer cell proliferation and inhibits apoptosis by silencing KLF2 and P21 expression. Mol Cancer Ther 2015; 14: 268-277.
11) Chen D, Zhang Z, Mao C, Zhou Y, Yu L, Yin Y, Wu S, Mou X, Zhu Y. ANRIL inhibits p15(INK4b) through the TGFbeta1 signaling pathway in human esophageal squamous cell carcinoma. Cell Immunol 2014; 289: 91-96.
12) Zou ZW, Ma C, Medoro L, Chen L, Wang B, Gupta R, Liu T, Yang XZ, Chen TT, Wang RZ, Zhang WJ, Li PD. LncRNA ANRIL is up-regulated in nasopharyngeal carcinoma and promotes the cancer progression via increasing proliferation, reprograming cell glucose metabolism and inducing side-population stem-like cancer cells. Oncotarget 2016; 7: 61741-61754.
13) Zhang D, Sun G, Zhang H, Tian J, Li Y. Long non-coding RNA ANRIL indicates a poor prognosis of cervical cancer and promotes carcinogenesis via PI3K/Akt pathways. Biomed Pharmacother 2017; 85: 511-516.
14) Zhao JJ, Hao S, Wang LL, Hu C Y, Zhang S, Guo LJ, Zhang G, Gao B, Jiang Y, Tian WG, Luo DL. Long non-coding RNA ANRIL promotes the invasion and metastasis of thyroid cancer cells through TGF-beta/Smad signaling pathway. Oncotarget 2016; 7: 57903-57918.
15) Holdt L M, Teupser D. From genotype to phenotype in human atherosclerosis--recent findings. Curr Opin Lipidol 2013; 24: 410-418.
16) Munz M, Richter GM, Loos B G, Jepsen S, Divaris K, Offenbacher S, Teumer A, Holtfreter B, Kocher T, Bruckmann C, Jockel-Schneider Y, Graetz C, Munoz L, Bhandari A, Tennstedt S, Staufenbiel I, van der Velde N, Uitterlinden AG, de Groot L, Wellmann J, Berger K, Krone B, Hoffmann P, Laudes M, Lieb W, Franke A, Dommisch H, Erdmann J, Schaefer A S. Genome-wide association meta-analysis of coronary artery disease and periodontitis reveals a novel shared risk locus. Sci Rep 2018; 8: 13678.
17) Schunkert H, Konig IR, Kathiresan S, Reilly MP, Assimes TL, Holm H, Preuss M, Stewart AF, Barbalic M, Gieger C, Absher D, Aherrahrou Z, Allayee H, Altshuler D, Anand SS, Andersen K, Anderson JL, Ardissino D, Ball SG, Balmforth A J, Barnes TA, Becker DM, Becker LC, Berger K, Bis JC, Boekholdt SM, Boerwinkle E, Braund PS, Brown MJ, Burnett MS, Buysschaert I, Cardiogenics, Carlquist JF, Chen L, Cichon S, Codd V, Davies RW, Dedoussis G, Dehghan A, Demissie S, Devaney JM, Diemert P, Do R, Doering A, Eifert S, Mokhtari NE, Ellis SG, Elosua R, Engert JC, Epstein S E, de Faire U, Fischer M, Folsom AR, Freyer J, Gigante B, Girelli D, Gretarsdottir S, Gudnason V, Gulcher JR, Halperin E, Hammond N, Hazen S L, Hofman A, Horne BD, Illig T, Iribarren C, Jones GT, Jukema JW, Kaiser MA, Kaplan LM, Kastelein JJ, Khaw KT, Knowles JW, Kolovou G, Kong A, Laaksonen R, Lambrechts D, Leander K, Lettre G, Li M, Lieb W, Loley C, Lotery AJ, Mannucci PM, Maouche S, Martinelli N, McKeown PP,

Meisinger C, Meitinger T, Melander O, Merlini P A, Mooser V, Morgan T, Muhleisen T W, Muhlestein JB, Munzel T, Musunuru K, Nahrstaedt J, Nelson CP, Nothen MM, Olivieri O, Patel RS, Patterson CC, Peters A, Peyvandi F, Qu L, Quyyumi AA, Rader DJ, Rallidis LS, Rice C, Rosendaal FR, Rubin D, Salomaa V, Sampietro ML, Sandhu MS, Schadt E, Schafer A, Schillert A, Schreiber S, Schrezenmeir J, Schwartz SM, Siscovick DS, Sivananthan M, Sivapalaratnam S, Smith A, Smith TB, Snoep JD, Soranzo N, Spertus JA, Stark K, Stirrups K, Stoll M, Tang WH, Tennstedt S, Thorgeirsson G, Thorleifsson G, Tomaszewski M, Uitterlinden AG, van Rij AM, Voight BF, Wareham NJ, Wells GA, Wichmann HE, Wild PS, Willenborg C, Witteman JC, Wright BJ, Ye S, Zeller T, Ziegler A, Cambien F, Goodall AH, Cupples LA, Quertermous T, Marz W, Hengstenberg C, Blankenberg S, Ouwehand WH, Hall AS, Deloukas P, Thompson J R, Stefansson K, Roberts R, Thorsteinsdottir U, O'Donnell C J, McPherson R, Erdmann J, Consortium CA, Samani NJ. Large-scale association analysis identifies 13 new susceptibility loci for coronary artery disease. Nat Genet 2011; 43: 333-338.

18) Bochenek G, Hasler R, El Mokhtari NE, Konig IR, Loos BG, Jepsen S, Rosenstiel P, Schreiber S, Schaefer AS. The large non-coding RNA ANRIL, which is associated with atherosclerosis, periodontitis and several forms of cancer, regulates ADIPOR1, VAMP3 and C11ORF10. Hum Mol Genet 2013; 22: 4516-4527.

19) Schaefer AS, Richter GM, Groessner-Schreiber B, Noack B, Nothnagel M, El Mokhtari NE, Loos B G, Jepsen S, Schreiber S. Identification of a shared genetic susceptibility locus for coronary heart disease and periodontitis. PLoS Genet 2009; 5: e1000378.

20) Xiong L, Liu W, Gao L, Mu Q, Liu X, Feng Y, Tang Z, Tang H, Liu H. The ANRIL genetic variants and their interactions with environmental risk factors on atherothrombotic stroke in a Han Chinese population. J Stroke Cerebrovasc Dis 2018; 27: 2336-2347.

21) Kral BG, Mathias RA, Suktitipat B, Ruczinski I, Vaidya D, Yanek LR, Quyyumi A A, Patel RS, Zafari AM, Vaccarino V, Hauser ER, Kraus WE, Becker LC, Becker DM. A common variant in the CDKN2B gene on chromosome 9p21 protects against coronary artery disease in Americans of African ancestry. J Hum Genet 2011; 56: 224-229.

22) Arslan S, Berkan O, Lalem T, Ozbilum N, Goksel S, Korkmaz O, Cetin N, Devaux Y, Cardiolinc n. Long non-coding RNAs in the atherosclerotic plaque. Atherosclerosis 2017; 266: 176-181.

23) Pasquinelli AE. MicroRNAs: heralds of the noncoding RNA revolution. RNA 2015; 21: 709-710.

24) Geisler S, Coller J. RNA in unexpected places: long non-coding RNA functions in diverse cellular contexts. Nat Rev Mol Cell Biol 2013; 14: 699-712.

25) Cesana M, Cacchiarelli D, Legnini I, Santini T, Sthandier O, Chinappi M, Tramontano A, Bozzoni I. A long noncoding RNA controls muscle differentiation by functioning as a competing endogenous RNA. Cell 2011; 147: 358-369.

26) Salmena L, Poliseno L, Tay Y, Kats L, Pandolfi PP. A ceRNA hypothesis: the Rosetta Stone of a hidden RNA language? Cell 2011; 146: 353-358.

27) Wu Z S, Wu Q, Wang CQ, Wang XN, Wang Y, Zhao JJ, Mao SS, Zhang GH, Zhang N, Xu X C. MiR-339-5p inhibits breast cancer cell migration and invasion *in vitro* and may be a potential biomarker for breast cancer prognosis. BMC Cancer 2010; 10: 542.

28) Zhou C, Liu G, Wang L, Lu Y, Yuan L, Zheng L, Chen F, Peng F, Li X. MiR-339-5p regulates the growth, colony formation and metastasis of colorectal cancer cells by targeting PRL-1. PLoS One 2013; 8: e63142.

29) Li Y, Zhang X, Yang Z, Li Y, Han B, Chen LA. MiR-339-5p inhibits metastasis of non-small cell lung cancer by regulating the epithelial-to-mesenchymal transition. Oncol Lett 2018; 15: 2508-2514.

30) Wang Y L, Chen C M, Wang XM, Wang L. Effects of miR-339-5p on invasion and prognosis of hepatocellular carcinoma. Clin Res Hepatol Gastroenterol 2016; 40: 51-56.

31) Shan W, Li J, Bai Y, Lu X. MiR-339-5p inhibits migration and invasion in ovarian cancer cell lines by targeting NACC1 and BCL6. Tumour Biol 2016; 37: 5203-5211.

32) Chen J, Cui X, Li L, Qu J, Raj JU, Gou D. MiR-339 inhibits proliferation of pulmonary artery smooth muscle cell by targeting FGF signaling. Physiol Rep 2017; 5(18). pii: e13441. doi: 10.14814/phy2.13441

33) Yang X, Liaw L, Prudovsky I, Brooks PC, Vary C, Oxburgh L, Friesel R. Fibroblast growth factor signaling in the vasculature. Curr Atheroscler Rep 2015; 17: 509.

34) Li Q, Teng Y, Wang J, Yu M, Li Y, Zheng H. Rap1 promotes proliferation and migration of vascular smooth muscle cell via the ERK pathway. Pathol Res Pract 2018; 214: 1045-1050.

35) Chen J, Dai M, Wang Y. Paeonol inhibits proliferation of vascular smooth muscle cells stimulated by high glucose via Ras-Raf-ERK1/2 signaling pathway in coculture model. Evid Based Complement Alternat Med 2014; 2014: 484269.

36) Chen HS, Tong HS, Zhao Y, Hong CY, Bin JP, Su L. Differential expression pattern of exosome long non-coding RNAs (lncRNAs) and microRNAs (miRNAs) in vascular endothelial cells under heat stroke. Med Sci Monitor 2018; 24: 7965-7974.

37) Hung J, Miscianinov V, Sluimer JC, Newby DE, Baker AH. Targeting non-coding RNA in vascular biology and disease. Front Physiol 2018; 9: 1655.

38) Voellenkle C, Garcia-Manteiga JM, Pedrotti S, Perfetti A, De Toma I, Da Silva D, Maimone B, Greco S, Fasanaro P, Creo P. Implication of long noncoding RNAs in the endothelial cell response to hypoxia revealed by RNA-sequencing. Sci Rep 2016; 6: 24141.

39) Yin K J, Hamblin M, Chen YE. Non-coding RNAs in cerebral endothelial pathophysiology: emerging roles in stroke. Neurochem Int 2014; 77: 9-16.

40) Kumar S, Williams D, Sur S, Wang JY, Jo H. Role of flow-sensitive microRNAs and long noncoding RNAs in vascular dysfunction and atherosclerosis. Vascul Pharmacol 2019; 114: 76-92.

41) Zhang W, Chen Y, Liu P, Chen J, Song L, Tang Y, Wang Y, Liu J, Hu FB, Hui R. Variants on chromosome 9p21.3 correlated with ANRIL expression contribute to stroke risk and recurrence in a large prospective stroke population. Stroke 2012; 43: 14-21.

42) Holdt LM, Beutner F, Scholz M, Gielen S, Gabel G, Bergert H, Schuler G, Thiery J, Teupser D. ANRIL expression is associated with atherosclerosis risk at chromosome 9p21. Arterioscler Thromb Vasc Biol 2010; 30: 620-627.

43) Congrains A, Kamide K, Katsuya T, Yasuda O, Oguro R, Yamamoto K, Ohishi M, Rakugi H. CVD-associated non-coding RNA, ANRIL, modulates expression of atherogenic pathways in VSMC. Biochem Biophys Res Commun 2012; 419: 612-616.

44) Yang J, Gu L, Guo X, Huang J, Chen Z, Huang G, Kang Y, Zhang X, Long J, Su L. LncRNA ANRIL expression and ANRIL gene polymorphisms contribute to the risk of ischemic stroke in the Chinese Han population. Cell Mol Neurobiol 2018; 38: 1253-1269.

45) Kotake Y, Nakagawa T, Kitagawa K, Suzuki S, Liu N, Kitagawa M, Xiong Y. Long non-coding RNA ANRIL is required for the PRC2 recruitment to and silencing of p15(INK4B) tumor suppressor gene. Oncogene 2011; 30: 1956-1962.

46) Yap KL, Li S, Munoz-Cabello AM, Raguz S, Zeng L, Mujtaba S, Gil J, Walsh MJ, Zhou MM. Molecular interplay of the noncoding RNA ANRIL and methylated histone H3 lysine 27 by polycomb CBX7 in transcriptional silencing of INK4a. Mol Cell 2010; 38: 662-674.

47) Pirillo A, Norata GD, Catapano AL. LOX-1, OxLDL, and atherosclerosis. Mediators Inflamm 2013; 2013: 152786.

48) Nakajima K, Nakano T, Tanaka A. The oxidative modification hypothesis of atherosclerosis: the comparison of atherogenic effects on oxidized LDL and remnant lipoproteins in plasma. Clin Chim Acta 2006; 367: 36-47.

49) Chistiakov DA, Orekhov AN, Bobryshev YV. Vascular smooth muscle cell in atherosclerosis. Acta Physiol (Oxf) 2015; 214: 33-50.

50) Johnson J L. Emerging regulators of vascular smooth muscle cell function in the development and progression of atherosclerosis. Cardiovasc Res 2014; 103: 452-460.

51) Smiljanic K, Obradovic M, Jovanovic A, Djordjevic J, Dobutovic B, Jevremovic D, Marche P, Isenovic ER. Thrombin stimulates VSMC proliferation through an EGFR-dependent pathway: involvement of MMP-2. Mol Cell Biochem 2014; 396: 147-160.

52) Fry J L, Shiraishi Y, Turcotte R, Yu X, Gao Y Z, Akiki R, Bachschmid M, Zhang Y, Morgan K G, Cohen R A, Seta F. Vascular smooth muscle sirtuin-1 protects against aortic dissection during angiotensin II-induced hypertension. J Am Heart Assoc 2015; 4: e002384.

53) Schlosser A, Pilecki B, Hemstra LE, Kejling K, Kristmannsdottir GB, Wulf-Johansson H, Moeller JB, Fuchtbauer EM, Nielsen O, Kirketerp-Moller K, Dubey LK, Hansen PB, Stubbe J, Wrede C, Hegermann J, Ochs M, Rathkolb B, Schrewe A, Bekeredjian R, Wolf E, Gailus-Durner V, Fuchs H, Hrabe de Angelis M, Lindholt J S, Holmskov U, Sorensen G L. MFAP4 promotes vascular smooth muscle migration, proliferation and accelerates neointima formation. Arterioscler Thromb Vasc Biol 2016; 36: 122-133.

54) Jin QS, Huang LJ, Zhao TT, Yao XY, Lin LY, Teng YQ, Kim SH, Nam MS, Zhang LY, Jin YJ. HOXA11-AS regulates diabetic arteriosclerosis-related inflammation via PI3K/AKT pathway. Eur Rev Med Pharmacol Sci 2018; 22: 6912-6921.

55) Li FP, Lin DQ, Gao LY. LncRNA TUG1 promotes proliferation of vascular smooth muscle cell and atherosclerosis through regulating miRNA-21/PTEN axis. Eur Rev Med Pharmacol Sci 2018; 22: 7439-7447.

56) Zhou X, Han X, Wittfeldt A, Sun J, Liu C, Wang X, Gan LM, Cao H, Liang Z. Long non-coding RNA ANRIL regulates inflammatory responses as a novel component of NF-kappaB pathway. RNA Biol 2016; 13: 98-108.

57) Chi J S, Li J Z, Jia J J, Zhang T, Liu X M, Yi L. Long non-coding RNA ANRIL in gene regulation and its duality in atherosclerosis. J Huazhong Univ Sci Technolog Med Sci 2017; 37: 816-822.

58) Guo F, Tang C, Li Y, Liu Y, Lv P, Wang W, Mu Y. The interplay of LncRNA ANRIL and miR-181b on the inflammation-relevant coronary artery disease through mediating NF-kappaB signalling pathway. J Cell Mol Med 2018; 22: 5062-5075.

59) Gotoh N. Regulation of growth factor signaling by FRS2 family docking/scaffold adaptor proteins. Cancer Sci 2008; 99: 1319-1325.

60) Muslin AJ. MAPK signalling in cardiovascular health and disease: molecular mechanisms and therapeutic targets. Clin Sci (Lond) 2008; 115: 203-218.

61) Minamino T, Yoshida T, Tateno K, Miyauchi H, Zou Y, Toko H, Komuro I. Ras induces vascular smooth muscle cell senescence and inflammation in human atherosclerosis. Circulation 2003; 108: 2264-2269.

62) Miura S, Matsuo Y, Saku K. Simvastatin suppresses coronary artery endothelial tube formation by disrupting Ras/Raf/ERK signaling. Atherosclerosis 2004; 175: 235-243.

63) Holdt LM, Stahringer A, Sass K, Pichler G, Kulak NA, Wilfert W, Kohlmaier A, Herbst A, Northoff BH, Nicolaou A, Gabel G, Beutner F, Scholz M, Thiery J, Musunuru K, Krohn K, Mann M, Teupser D. Circular non-coding RNA ANRIL modulates ribosomal RNA maturation and atherosclerosis in humans. Nat Commun 2016; 7: 12429.

64) Mahmoud SSE, Ismail NA, Farag YM, Hashem RH, Ibrahim MH, Salah MM, Tous AN. Intima media thickness as an early predictor of atherosclerosis in Egyptian children with familial Mediterra-

nean fever. Arch Med Sci Atheroscler Dis 2018; 3: e106-e111.

65) Zhu X, Zhao P, Lu Y, Huo L, Bai M, Yu F, Tie Y. Potential injurious effects of the fine particulate PM2.5 on the progression of atherosclerosis in apoE-deficient mice by activating platelets and leukocytes. Arch Med Sci 2019; 15: 250-261.

66) Dziedzic EA, Gasior JS, Pawlowski M, Wodejko-Kucharska B, Saniewski T, Marcisz A, Dabrowski MJ. Vitamin D level is associated with severity of coronary artery atherosclerosis and incidence of acute coronary syndromes in non-diabetic cardiac patients. Arch Med Sci 2019; 15: 359-368